Experimental EKF-based SLAM for mini-rovers with IR sensors only

Fabrizio Abrate* Basilio Bona* Marina Indri*
*Dipartimento di Automatica e Informatica, Politecnico di Torino,
Corso Duca degli Abruzzi 24, 10129 Torino, Italy
e-mail: fabrizio.abrate@polito.it, basilio.bona@polito.it, marina.indri@polito.it

***Abstract*— The performances of an EKF-based SLAM approach are experimentally discussed in the case of a mini-robot equipped with low-cost IR sensors only, showing that despite of the sparseness and noisiness of the sensors, SLAM experiments using classical SLAM methods can be performed even on a Khepera robot in a real arena, whose dimensions may be significantly larger than the robot size. The main characteristics of the SLAM approach and of the used sensors are described in the paper, which illustrates and discusses the performed tests and their results.**

***Index Terms*— SLAM, IR sensors, Sparse Sensing.**

I. Introduction

Small mobile robots are becoming part of the everyday life, as robotic assistants in many real-life situations, for security monitoring purposes, for rescue operations and for entertainment. Moreover, many universities and high schools all over the world intensively use mini robots for educational purposes, since they are small, low-cost devices that can offer various opportunities to address control and hardware/software issues, together with electronics, sensors and power consumption aspects.

The main characteristic that is required from such consumer-oriented robots is a strong autonomy. One of the most interesting problems, specifically oriented to enhance the autonomy of a mobile robot, is surely represented by Simultaneous Localization And Mapping (SLAM), which would give the possibility to place an autonomous vehicle at an unknown location in an unknown environment, build a map using only relative observations of the environment, and then simultaneously use this map to navigate, thus eliminating any need for artificial landmarks to guide the robot motion, or for an a-priori topological knowledge of the environment.

The SLAM problem has been intensively studied over the last years [5]-[7], [13], [15], [17], [19] even if a definite, fully satisfying solution still remains a sort of "Holy Grail" for the autonomous vehicle research community. The dominant approach to the SLAM problem was introduced in a seminal paper by Smith, Self, and Cheeseman [16]. This paper proposed the use of the Extended Kalman Filter (EKF) to incrementally estimate the joint posterior distribution over robot pose and landmark positions. Most recent SLAM works have been focused on creating accurate maps using laser rangefinders either to extract features from the environment [18] or to perform scan matching against the robot map [8]. The particle filtering approach for SLAM has recently gained wide acceptance, and both landmark and scanmatching based techniques have been developed on the basis of the strategy of Rao-Blackwellized particle filtering, as shown in [4] and [14].

It must be stressed that the most relevant proposed solutions require the use of expensive and high quality sensors; only in few cases the SLAM problem was addressed under sensing constraints such as sensor sparseness, range limitations and significant noise affecting the acquired data. In the topological mapping domain, Huang and Beevers [10], [11] have developed a complete algorithm to trace a version of the Voronoi diagram of a rectilinear environment using eight radially spaced short-range sensors. In [3] an efficient approach to enable SLAM in indoor environments is proposed for robots with much more limited sensing than a laser rangefinder. In practice they decimate the acquired data coming from the Radish repository [9] maintaining only 5 measures per scan and reducing the range to 5 m. A further reference for SLAM with mini-robots is given by [12], where vision is used to recognize places and then odometry to derive a metrical link between these places.

Since the most common mini-rovers are usually endowed with low-cost sensors only, such as InfraRed (IR) sensors, often mounted in a sparse configuration, in this paper we experimentally show how SLAM can be performed by classical methods in an indoor-like environment with robots having limited, sparse and really noisy sensing following a multiscan approach similar to the one applied in [20] and [21], where sonar data taken from multiple locations were used to extract features and perform SLAM. It must be noted that small laser rangefinders have been recently produced, but they have not been embedded in mini-robots yet, mainly because of their large power consumption, which may rapidly discharge the batteries of such small robots. This paper is then also aimed at identifying and clarifying the application frontiers of mini-robots.

The paper is organized as follows: Section II introduces the SLAM approach, drawing its main characteristics; Section III illustrates the experimental framework, describing in particular the IR sensors embedded in the Khepera II© robot used for the experiments. Section IV describes the arena built for the tests, whose results are reported and discussed in Section V. Section VI draws some final conclusions.

II. The SLAM approach

The developed SLAM approach can be basically summarized in the following three main steps:

- line extraction;
- data association;
- Extended Kalman Filtering (EKF).

We have decided to implement a *line extraction* step because of the specific characteristics of the environment we have

considered, made only of straight walls and corners, as can be seen in Section IV.
The main theoretical characteristics of each step are briefly recalled in the remainder of this Section.

A. Line Extraction

While moving, the rover collects data with its IR sensors. The line extraction step starts when a sufficient number of measures have been collected. Such a step allows the extraction of n line features of the environment from the raw data acquired by the IR sensors at every iteration of the algorithm. Considering a single iteration of the algorithm, two sub-steps are applied:

1) A *segmentation* step is performed by initially applying a sliding window of $a = 5$ measures on the l available measures, expressed in polar coordinates. After this step, l groups of a measures are obtained; then a non-linear fit is performed on each group in order to obtain l straight lines represented according to the *Hessian line model* (see Appendix B in [2]). These lines constitute the very first set of candidates that can become the *recognized features* of the environment; then, the algorithm tries to identify some *regions* wherein certain lines can be fused. The criterion for identifying the regions is the computation of a *compactness* index for every group of $b = 3$ adjoining lines. In particular, we denote with h_i, with $i = 1, \ldots, l$, every group of b adjoining Hessian lines, where the index i refers to the central line of the group. Next an *Information Filter* is computed for every group, using the equations below:

$$\overline{C}_{h_i} = \left(\sum_{j=i-1}^{i+1} C_j^{-1} \right)^{-1} \tag{1a}$$

$$\overline{x}_{h_i} = \overline{C}_{h_i} \sum_{j=i-1}^{i+1} C_j^{-1} x_j \tag{1b}$$

where each x_i contains the Hessian line parameters

$$x_i = \begin{bmatrix} \alpha_i \\ r_i \end{bmatrix} \tag{2}$$

and each C_i is the 2×2 covariance matrix of the Hessian lines

$$C_i = \begin{bmatrix} c_{\alpha_i \alpha_i} & c_{\alpha_i r_i} \\ c_{r_i \alpha_i} & c_{r_i r_i} \end{bmatrix} \tag{3}$$

After that, l compactness indexes are computed as the sum of the Mahalanobis distances of the considered lines in h_i, using the following expression:

$$d_{h_i} = \sum_{j=i-1}^{i+1} (x_j - \overline{x}_{h_i})^T (C_j + \overline{C}_{h_i})^{-1} (x_j - \overline{x}_{h_i}) \tag{4}$$

Finally a threshold is applied in order to determine which groups have to be fused in a new region; the measurements belonging to the new regions are fitted in order to obtain new Hessian lines; these lines can be considered as small clusters.

2) A *hierarchical clustering* algorithm is applied in order to fuse the segments that belong to the same physical object (e.g. a wall), even if they appear as different.

B. Data Association

Data association is the process of making correspondences between previously observed features and a new one, locally observed while the rover moves and the SLAM algorithm iterates. It is a very important step, since wrong associations of features cannot guarantee the map consistency and the algorithm convergence.

In this work we have implemented a *Nearest Neighbor Standard Filter* (NNSF) [2]. The data validation process is performed comparing the *Normalized Innovation Squared* (NIS), computed for every possible pair of one local and one global feature, as follows

$$v_{ij}^T S_{ij}^{-1} v_{ij} < d_{min} \tag{5}$$

where v_{ij} is the innovation vector between the i-th and the j-th feature, and S_{ij} is the covariance of v_{ij} with a *validation gate* d_{min} coming from a χ^2 distribution having the same dimension as the innovation vector (it is 2 in our case). If the value of the *validation gate* is high, a big percentage of feature matching candidates is considered as correct. We have decided to select a high value to maximize the feature matching. In this case the ambiguity of the association increases, but experimentally we have noticed that high values perform better than low values.

C. The EKF

The filter that has been chosen to perform the state estimation in the SLAM experiments is the Extended Kalman Filter (EKF), i.e., the Kalman filter linearized by the first term of a Taylor expansion around the estimated quantities. One of the main problems of EKF is that the determination of the full covariance matrix is computationally heavy, making the real-time SLAM unfeasible when the number of features is really high, and increases rapidly over time.
In our approach, however, the *Line Extraction* ad *Data Association* procedures are designed so that the number of features locally identified from a set of raw data is very small at each iteration. In this way the full covariance matrix can be easily computed, overcoming one of the main limitations of EKF filtering.

III. The Rover and its Sensors

The experimental study of the possibility of performing Simultaneous Localization and Mapping, using a robot equipped with low-cost IR sensors only, has been carried out with reference to the Khepera II© robot in a real arena. In the following, we introduce the main features of the Khepera II© robot, and of its IR sensors in particular.

A. Khepera II©

The Khepera II© robot is a non-holonomic differential drive mobile robot. It embeds a 25 MHz Motorola© 68331 processor with 512 kBytes RAM memory and 512 kBytes programmable Flash memory. The robot is moved by 2 DC brushed servo motors with incremental encoders, that can drive the robot from a minimum velocity of 0.02 m/s up to a maximum of 0.6 m/s. The robot is quite small and light, since its diameter is 0.07 m, its axle length is 0.053 m, its height

is 0.03 m and it weights only 0.8 kg. It is equipped with 8 IR proximity sensors with up to 0.05 m range; the sensors disposition can be seen in Figure 1.

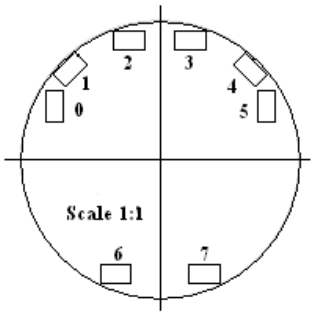

Fig. 1. The position of the 8 Infra-Red sensors

B. The IR sensors characteristics

In general IR sensors are small devices that can emit an infrared light ray and sense the presence of an object using the IR-beam reflected from the object itself. IR sensors are often found in *optoelectronic scanning* and *switching devices*, i.e., index sensing and coded disk scanning. Considering the robotics field and especially mobile robotics, IR sensors have often been used as *proximity sensors*, with the task of detecting obstacles. In this work the IR sensors will be used to measure the distances from the perceived obstacles. This is a non-trivial issue, because previous experiments performed with walls covered with white reflective paper revealed that the measurements uncertainty is approximately 15 mm, a huge value with respect to the maximum detectable distance, which is 50 mm.

In [1] two different ways of modelling IR sensors are proposed. In this work we do not explicitly model the sensor behavior in any specific way, but we only adopt the characteristic shown in Figure 2. It is easy to see that, performing a linear fitting, the linearity interval would be too small (nearly only 10 mm). This would force the robot to keep, while travelling, distances not greater than 10 mm from the wall to let the sensors acquire reliable data, but in this way even small motion errors could result in collision with obstacles. Therefore, we fitted the data with a 5-th order polynomial, in order to allow the sensors to acquire data in a larger interval (nearly 40 mm).

IV. The arenas for the tests

The arena that has been built to perform the SLAM experiments can be seen in Figure 3 (a), while the features to be identified by the robot are shown in the map of the arena built using Matlab©, reported in Figure 3 (b).

The 2m $\times$ 1m arena is big compared to the diameter of the Khepera II robot, and it is quite simple and regular from the geometric point of view. However it can be considered a good test-bench for the SLAM approach, in particular in determining the precision of the corners estimation. The walls of the arena are made of paperboard covered with white reflective paper.

In Figure 3 (b) the labels $S_1, \ldots, S_{21}$ indicate the 21 true line

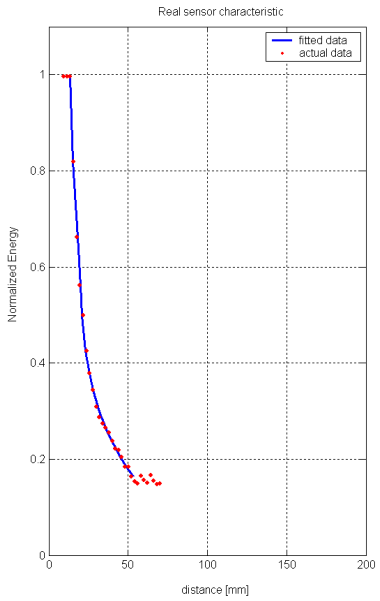

Fig. 2. The sensors characteristic

TABLE I
Hessian parameters of the true features for Test 3

	S_1	S_2	S_3	S_4	S_5	S_6	S_7
α [degrees]	270	0	270	180	180	90	180
r [mm]	40	200	390	100	400	260	500
	S_8	S_9	S_{10}	S_{11}	S_{12}	S_{13}	S_{14}
α [degrees]	90	180	90	0	90	0	90
r [mm]	460	60	1160	500	960	240	560
	S_{15}	S_{16}	S_{17}	S_{18}	S_{19}	S_{20}	S_{21}
α [degrees]	0	90	270	270	90	90	90
r [mm]	400	160	590	840	690	710	860

features that identify the various walls in the arena. In Table I the true α and r Hessian values of the features are reported with respect to the reference frame *Ref 1* of Figure 3(b).

V. Experimental results

Several tests have been performed in order to prove the feasibility of our SLAM application and to understand its peculiarities and limitations: the most significant ones are reported and discussed hereafter.

A. Test 1

The first test has been performed to check the behavior of the IR sensors; the robot, while moving around a rectangular obstacle, tries to identify the features that represent the obstacle itself.

The experiment is shown in Figure 4, where the red segments represent the portion of the Hessian straight lines computed by the algorithm while the mini-rover moves. Considering the simple visual inspection as evaluation criterion, the result of this initial test seems quite satisfactory and encouraging for more complex tests.

(a)

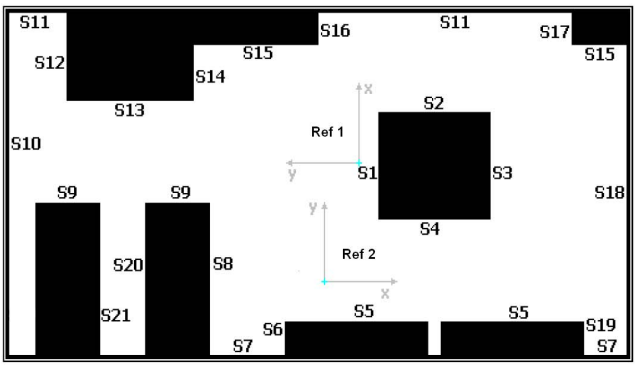

(b)

Fig. 3. The real arena (a) and its grid map representation (b)

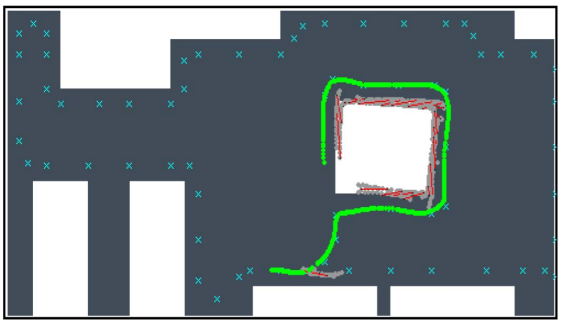

Fig. 4. Test 1

B. Test 2

In the second test the robot explores the full perimeter of the arena by moving along a preconditioned path through a set of way points.

As can be seen in Figure 5, the result is not satisfactory, especially when looking at the portion included in the yellow oval, because there are few data acquired and these data are very inaccurate. This leads to a lack of information that prevents to build a significant map of the environment.

The failure of the experiment is basically due to the high distance of the robot from the obstacles and to the absence of lateral sensors.

The high distance has a double adverse effect. On the one hand, if an IR sensor perceives an obstacle that is too far, the estimation error increases, adversely affecting the update

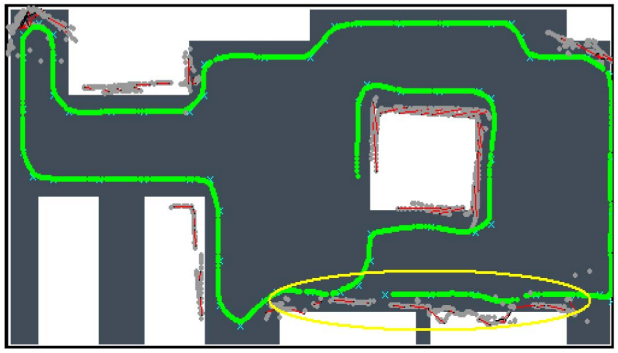

Fig. 5. Test 2

phase of the EKF-algorithm. On the other hand, if an obstacle is too far and cannot be perceived, the feature detection process does not occur, causing the map impoverishment and the accumulation of odometry errors due to the absence of the SLAM update feedback.

C. Test 3

In this test we choose the robot path in such a way that the obstacles are always in the field view of the sensors, and we expect better performances than the ones obtained in Test 2. The segments revealed by the algorithm are highlighted

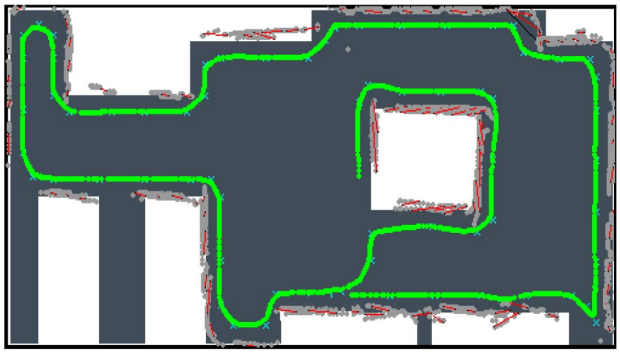

Fig. 6. Test 3

in Figure 6. The r and α estimated values of the features are reported in Table II, while Figures 7 and 8 compare the estimated values for r and α with the true ones of Table I.

TABLE II

HESSIAN PARAMETERS OF THE ESTIMATED FEATURES IN TEST 3

	$\hat{S}_1$	$\hat{S}_2$	$\hat{S}_3$	$\hat{S}_4$	$\hat{S}_5$	$\hat{S}_6$	$\hat{S}_7$
α [degrees]	265.5	-5.5	277	263.4	175.4	178.9	175.3
r [mm]	48.1	215.8	457.1	401.9	82.6	404.4	529.6
	$\hat{S}_8$	$\hat{S}_9$	$\hat{S}_{10}$	$\hat{S}_{11}$	$\hat{S}_{12}$	$\hat{S}_{13}$	$\hat{S}_{14}$
α [degrees]	89.3	179.9	90.3	6.2	96.5	-5.2	-5.3
r [mm]	513.9	56.8	1158.1	637.1	921.9	187	374.2
	$\hat{S}_{15}$	$\hat{S}_{16}$	$\hat{S}_{17}$	$\hat{S}_{18}$	$\hat{S}_{19}$	$\hat{S}_{20}$	$\hat{S}_{21}$
α [degrees]	26.7	11.2	148.8	271.7	264.3	164.9	164.9
r [mm]	471	491.5	680.8	610.3	826.9	230.1	405

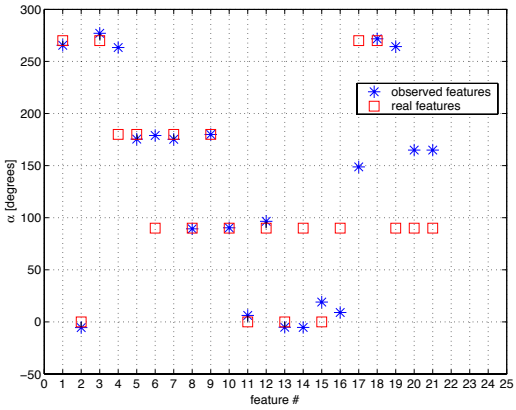

Fig. 7. Observed and real features in Test 3 (α values)

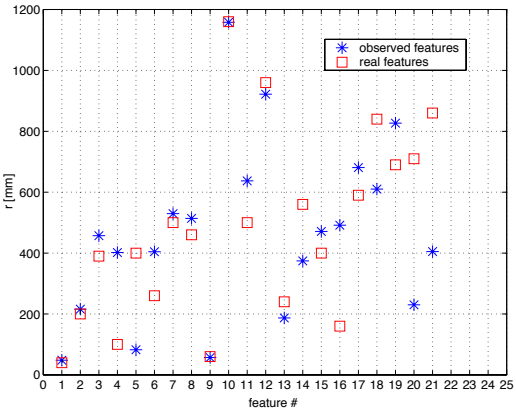

Fig. 8. Observed and real features in Test 3 (r values)

The overall result can be considered satisfactory, showing that if the robot travels along a suitable path, the EKF-based SLAM is consistent.
The graph of Figure 7 shows the α real and estimated values. Only some features are badly estimated, such as S_4, S_6, S_{14} and the last three ones, because the robot estimates them only on the basis of a corner detection, which is particularly critical for the noisy IR sensors. The graph of Figure 8 shows instead the r real and estimated values. The estimation error is small for most of the features, showing that the *line extraction* phase has been designed properly.

Taking into account the sensors inaccuracy, the overall mapping reconstruction can be surely considered as acceptable, even if some segments, associated with the most critical features, are uncorrect, as shown in Figure 6.

D. Test 4

It is impossible in a realistic scenario to accurately plan the path of a robot, since it has to move in a totally unknown environment. Therefore a further test has been performed in order to show that, even if the robot does not travel along the optimal path and encounters the obstacles in a different order with respect to Tests 2 and 3, the resulting map can be satisfactory. By the term "optimal path", we intend a path that maximizes the possibility of accurately detecting the obstacles in order to increase the SLAM performances. The robot in this experiment travels along the path counterclockwise with respect to Tests 2 and 3 (see Figure 9), starting from the origin of *Ref 2* shown in Figure 3(b), so the order in which the true features are encountered changes: in Table III the true α and r Hessian values of the features are reported with respect to the reference frame *Ref 2* of Figure 3(b).

Fig. 9. Test 4

TABLE III
HESSIAN PARAMETERS OF THE TRUE FEATURES IN TEST 4

	S_1	S_2	S_3	S_4	S_5	S_6	S_7
α [degrees]	0	90	0	90	270	180	270
r [mm]	160	560	550	260	40	100	140
	S_8	S_9	S_{10}	S_{11}	S_{12}	S_{13}	S_{14}
α [degrees]	180	90	180	90	180	90	180
r [mm]	300	300	1000	860	800	610	400
	S_{15}	S_{16}	S_{17}	S_{18}	S_{19}	S_{20}	S_{21}
α [degrees]	90	0	0	0	0	180	180
r [mm]	760	0	750	1000	850	550	700

The r and α estimated values for each feature and the comparison with the true ones are reported in Table IV and in Figures 10 and 11, respectively. There are some features missing indicated as N.O. (Not Observed) in Table IV. In particular, the first four features are not observed because the robot does not explore the rectangular obstacle, as done in Test 3; the other N.O. features are simply not sensed by the rover. As Figures 10 and 11 show, both the α and r estimation errors are limited in this case too, at least for the observable features, even if the path has changed and it has no more been planned in order to optimize the sensor detection capability.

VI. CONCLUSIONS

The experimental tests have shown the importance of the sensor characteristics to obtain satisfactory results in a SLAM problem. The most common mini-robots in their base configuration, like the Khepera II© used in our tests, are often equipped only with low-cost IR sensors that can be successfully used as proximity sensors for obstacle detection, but that are only partially suitable for distance measurements. In spite of their limited range, sparseness and noisiness, we have shown that quite satisfactory results can be achieved by

TABLE IV

HESSIAN PARAMETERS OF THE ESTIMATED FEATURES IN TEST 4

	$\hat{S}_1$	$\hat{S}_2$	$\hat{S}_3$	$\hat{S}_4$	$\hat{S}_5$	$\hat{S}_6$	$\hat{S}_7$
α [degrees]	N.O.	N.O.	N.O.	N.O.	263.6	N.O.	276.9
r [mm]	N.O.	N.O.	N.O.	N.O.	32.3	N.O.	106.2
	$\hat{S}_8$	$\hat{S}_9$	$\hat{S}_{10}$	$\hat{S}_{11}$	$\hat{S}_{12}$	$\hat{S}_{13}$	$\hat{S}_{14}$
α [degrees]	156	284	174.1	102.5	190.8	96.4	195.5
r [mm]	328.1	497.5	1081.2	854.9	840.4	661.7	353.4
	$\hat{S}_{15}$	$\hat{S}_{16}$	$\hat{S}_{17}$	$\hat{S}_{18}$	$\hat{S}_{19}$	$\hat{S}_{20}$	$\hat{S}_{21}$
α [degrees]	96.2	N.O.	7.5	5.5	N.O.	171.4	N.O.
r [mm]	800.1	N.O.	707.5	996.8	N.O.	471.6	N.O.

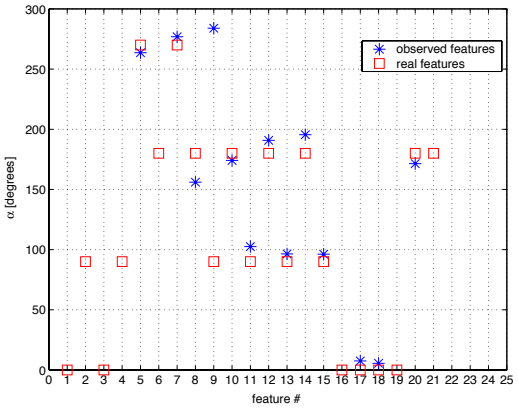

Fig. 10. Observed and real features in Test 4 (α values)

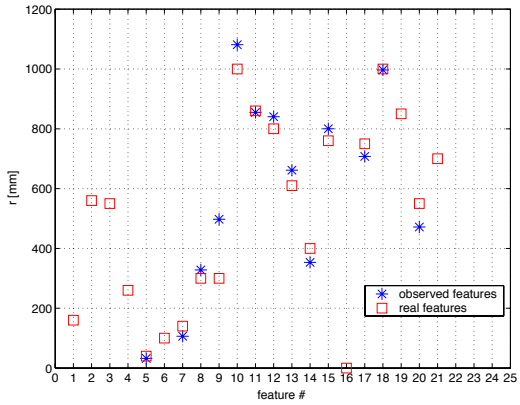

Fig. 11. Observed and real features in Test 4 (r values)

the application of an EKF-based SLAM approach, even if the arena in which the robot moves is big with respect to the robot dimensions. The success of the approach is mainly due to the efficiency of the associated use of the *line extraction* and *data association* procedures. It must be stressed that the performances can strongly depend on the chosen path, which must somehow help the sensor capabilities to reduce the number of unobservable features.

ACKNOWLEDGMENT

The authors thank Giada Grimaldi for her invaluable help in the experimental tests.

REFERENCES

[1] F. Abrate, M. Indri, and B. Bona, "Monte Carlo Localization of mini-rovers with low-cost IR sensors," in *IEEE/ASME Int Conf. On Advanced Intelligent Mechatronics (AIM)*, 2007.

[2] K. H. Arras, "Feature-based robot navigation in known and unknown environments," in *Phd thesis*, 2003.

[3] K. Beevers and W. Huang, "Slam with sparse sensing," in *Proceedings 2006 IEEE International Conference on Robotics and Automation (ICRA 2006)*, 2006, pp. 2285–2290.

[4] A. Doucet, N. de Freitas, K. Murphy, and S. Russell, "Rao-blackwellised particle filtering for dynamic bayesian networks," in *Conference on Uncertainty in Artificial Intelligence (UAI)*, 2000.

[5] H. Durrant-Whyte, D. Rye, and E. Nebot, "Concurrent localization and map building for mobile robots using ultrasonic sensors," in *IEEE Int. Workshop Intell. Robots Syst. (IROS)*, 1993.

[6] H. Durrant-Whyte, D. Rye, and E. Nebot, "Localisation of automatic guided vehicles," in *Robotics Research: The 7th International Symposium (ISRR95), G. Giralt and G. Hirzinger, Eds. New York: Springer Verlag*, 1996, pp. 613–625.

[7] H. Durrant-Whyte, "Uncertain geometry in robotics," *IEEE Trans. Robot. Automat.*, vol. 4, no. 1, pp. 23–31, 1988.

[8] G. Grisetti, C. Stachniss, and W. Burgard, "Improving gridbased slam with rao-blackwellized particle filters by adaptive proposals and selective resampling," in *Proc. of the IEEE Intl. Conf. on Robotics and Automation*, 2005, pp. 2443–2448.

[9] A. Howard and N. Roy, "The robotics data set repository (radish)," 2003.

[10] W. H. Huang and K. R. Beevers, "Topological mapping with sensing-limited robots," *Algorithmic Foundations of Robotics VI, Springer*, pp. 235–250, 2005.

[11] W. H. Huang and K. R. Beevers, "Complete topological mapping with sparse sensing," *Technical Report 05-06*, Rensselaer Polytechnic Institute, Troy, 2005.

[12] W. Hübner, "From homing behavior to cognitive mapping integration of egocentric pose relations and allocentric landmark information in a graph model," Ph.D. dissertation, Universität Tübingen, 2004.

[13] J. Leonard and H. Durrant-Whyte, "Directed sonar navigation," *Norwell, MA: Kluwer*, 1992.

[14] K. Murphy and S. Russell, "Rao-blackwellized particle filtering for dynamic bayesian networks," *Sequential Monte Carlo Methods in Practice,Springer*, 2001.

[15] R. Smith and P. Cheesman, "On the representation of spatial uncertainty," *Int. J. Robot. Res.*, vol. 5, no. 4, pp. 56–68, 1987.

[16] R. Smith, M. Self, and P. Cheeseman, "Estimating uncertain spatial relationships in robotics," *Autonomous Robot Vehicles,Springer*, 1990.

[17] S. Thrun, D. Fox, and W. Burgard, "A probabilistic approach to concurrent mapping and localization for mobile robots," *Mach. Learning*, vol. 31, no. 1, pp. 29–53, 1998.

[18] S. Thrun, M. Montemerlo, D. Koller, B. Wegbreit, J. Nieto, and E. Nebot, "Fastslam: An efficient solution to the simultaneous localization and mapping problem with unknown data association," *Journal of Machine Learning Research*, 2004. [Online]. Available: http://www.thrun.org/papers/Thrun03g.html

[19] S. Thrun, W.Burgard, and D. Fox, *Probabilistic Robotics*. MIT Press, 2005.

[20] O. Wijk and H. Christensen, "Triangulation based fusion of sonar data with application in robot pose tracking," *IEEE Transactions on Robotics and Automation*, vol. 16(6), pp. 740–752, 2000.

[21] G. Zunino and H. Christensen, "Navigation in realistic environments," in *Proc. 9th Intl. Symp. on Intelligent Robotic Systems (M. Devy, editor)*, 2001.